EBioMedicine 10 (2016) 71–76

Contents lists available at ScienceDirect

EBioMedicine

journal homepage: www.ebiomedicine.com

Research Paper

Comparative Analysis Between Flaviviruses Reveals Specific Neural Stem Cell Tropism for Zika Virus in the Mouse Developing Neocortex

Jean-Baptiste Brault [a], Cécile Khou [b], Justine Basset [b,1], Laure Coquand [a,1], Vincent Fraisier [a], Marie-Pascale Frenkiel [b], Bruno Goud [a], Jean-Claude Manuguerra [b], Nathalie Pardigon [b,2], Alexandre D. Baffet [a,*,2]

[a] Institut Curie, PSL Research University, CNRS, UMR144, F-75005 Paris, France
[b] Institut Pasteur, ERI/CIBU Arbovirus Group, 25 rue du Dr Roux, 75015 Paris, France

ARTICLE INFO

Article history:
Received 23 June 2016
Received in revised form 6 July 2016
Accepted 14 July 2016
Available online 16 July 2016

ABSTRACT

The recent Zika outbreak in South America and French Polynesia was associated with an epidemic of microcephaly, a disease characterized by a reduced size of the cerebral cortex. Other members of the *Flavivirus* genus, including West Nile virus (WNV), can cause encephalitis but were not demonstrated to cause microcephaly. It remains unclear whether Zika virus (ZIKV) and other flaviviruses may infect different cell populations in the developing neocortex and lead to distinct developmental defects. Here, we describe an assay to infect mouse E15 embryonic brain slices with ZIKV, WNV and dengue virus serotype 4 (DENV-4). We show that this tissue is able to support viral replication of ZIKV and WNV, but not DENV-4. Cell fate analysis reveals a remarkable tropism of ZIKV infection for neural stem cells. Closely related WNV displays a very different tropism of infection, with a bias towards neurons. We further show that ZIKV infection, but not WNV infection, impairs cell cycle progression of neural stem cells. Both viruses inhibited apoptosis at early stages of infection. This work establishes a powerful comparative approach to identify ZIKV-specific alterations in the developing neocortex and reveals specific preferential infection of neural stem cells by ZIKV.

1. Introduction

First isolated in 1947 from the blood of a Rhesus monkey in the Zika forest, Uganda (Dick et al., 1952), Zika virus (ZIKV) was recently declared a global public health emergency by WHO (Heymann et al., 2016). After decades of confinement in Africa and Asia, the first large outbreak caused by the virus was recorded in French Polynesia in 2013 (Cao-Lormeau et al., 2014), leading to an unusual increase in the number of Guillain-Barré cases (Paixão et al., 2016). The current South-American epidemic which started in 2015 in Brazil revealed a strong correlation between infection with ZIKV and congenital brain malformations, including microcephaly (Oliveira Melo et al., 2016).

Microcephaly is characterized by smaller head circumference, intellectual disability and seizures, and is due to reduced neuronal production or increased cell death (Barkovich et al., 2012). Recent data strongly supports the link between ZIKV and microcephaly, including detection of the virus in the amniotic fluid, placenta and brain of microcephalic fetuses, as well as in the blood of microcephalic newborns (Calvet et al., 2016; Mlakar et al., 2016; Martines et al., 2016). A retrospective study recently revealed a similar association between the French Polynesian 2013 outbreak and increased rates of microcephaly, supporting the implication of ZIKV (Cauchemez et al., 2016).

ZIKV belongs to the *Flavivirus* genus and is closely related to yellow fever virus (YFV), dengue virus (DENV), West Nile virus (WNV) and Japanese encephalitis virus (JEV). Flaviviruses are arthropod-borne, single-stranded positive-sense RNA viruses, that cause infections in humans with a spectrum of clinical syndromes ranging from mild fever to hemorrhagic and encephalitic manifestations. Several infectious agents, belonging to the so-called TORCH complex, are responsible for congenital infections leading to brain developmental disorders, including microcephaly (Neu et al., 2015). However, neurotropic flaviviruses such as WNV and JEV, responsible for post-natal encephalitis, are rarely linked to congenital brain malformations, such as microcephaly (O'Leary et al., 2006; Chaturvedi et al., 1980). Thus, neurovirulence of ZIKV in human fetuses must rely on mechanisms that are different from those involved in WNV or JEV neural infection, for example by infecting a particular set of fetal cells.

The cerebral cortex, a layered structure involved in higher cognitive functions, is strongly affected in microcephalic patients (Barkovich et al., 2012). During its normal development, all cortical neurons and most glial cells are generated, directly or indirectly, by the radial glial

* Corresponding author.
E-mail address: alexandre.baffet@curie.fr (A.D. Baffet).
[1] The third and fourth authors equally contributed to this study.
[2] Shared last authorship.

http://dx.doi.org/10.1016/j.ebiom.2016.07.018

progenitor (RGP) cells (Kriegstein and Alvarez-Buylla, 2009). These cells are highly polarized and elongated, spanning the entire thickness of the developing neocortex. The apical process of RGP cells is in contact with the ventricular surface and the cerebro-spinal fluid (CSF), while their basal process is in contact with the pial surface and serves as a track for neuronal migration (Taverna et al., 2014). Genetic alterations leading to microcephaly are well known to affect RGP cell division, fate or survival (Fernández et al., 2016).

In vitro studies using induced Pluripotent Stem Cells (iPSCs)-derived brain cells, neurospheres and brain organoids have shown ZIKV infection of human neural stem and progenitor cells (Tang et al., 2016; Garcez et al., 2016; Qian et al., 2016; Dang et al., 2016). Recently, two different mouse models for ZIKV infection were developed and revealed a range of development defects including placental damage, developmental delay, ocular defects and embryonic death (Cugola et al., 2016; Miner et al., 2016). Another study described RGP cell infection and reduced cortical thickness after ZIKV injection into the lateral ventricle of embryonic brains (Li et al., 2016). It remains unclear if RGP cell infection was merely due to their location at the site of virus injection or if ZIKV has a specific tropism for these cells in the developing neocortex. This question is particularly important as it is still unknown if the virus reaches the developing brain *via* the cerebrospinal fluid (CSF), where ZIKV was detected (Rozé et al., 2016), or *via* blood vessels after crossing the placenta, as recently suggested (Miner et al., 2016). Another outstanding question is whether all flaviviruses share similar characteristics of infection in the developing brain, or if ZIKV, and especially microcephaly-associated ZIKV, exhibits a specific behavior in this tissue. In view of the rare congenital abnormalities associated with other flaviviruses, including following intrauterine WNV infection (O'Leary et al., 2006), a comparative analysis between flaviviruses should provide a framework to identify ZIKV-specific mechanisms leading to microcephaly.

2. Materials & Methods

2.1. Flavivirus Production

2.1.1. Cells

Rhesus monkey Vero NK kidney cells were maintained at 37 °C in Dulbecco's modified Eagle medium (DMEM) supplemented with 5% FBS. *Aedes albopictus* C6/36 cells were maintained at 28 °C in L15 medium supplemented with 10% FBS.

2.1.2. Virus Stock

DENV-4 strain 63632/76 (Burma) was produced in C6/36 cells. WNV strain IS98 was produced as described in (Alsaleh et al., 2016). ZIKV strain Pf13 was isolated from a viremic patient in French Polynesia in 2013 by the team of V. M. Cao-Lormeau and D. Musso at the Institut Louis Malardé in French Polynesia (Cao-Lormeau et al., 2014). To produce viral stocks, C6/36 cells were infected with ZIKV strain Pf13 at an MOI of 0.1 and supernatants were harvested 5 days post-infection at the onset of cytopathic effect.

2.1.3. Titration

Vero NK cells were seeded in 24-well plates. Tenfold dilutions of virus samples were prepared in DMEM and 200 μL of DMEM supplemented with 2% FBS and 200 μL of each dilution were added to the cells. The plates were incubated for 1 h 30 min at 37 °C. Unadsorbed virus was removed, after which 400 μL of DMEM supplemented with 2% FBS and 400 μL of DMEM supplemented with 1.6% carboxymethyl cellulose (CMC), 10 mM HEPES buffer, 72 mM sodium bicarbonate, and 2% FBS was added to each well, followed by incubation at 37 °C for 72 h for ZIKV and WNV, and for 96 h for DENV-4. The CMC overlay was aspirated, and the cells were washed with PBS and fixed with 4% paraformaldehyde for 20 min, followed by permeabilization with 0.1% Triton X-100 for 5 min. After fixation, the cells were washed with PBS and incubated for 1 h at room temperature with anti-E antibody (4G2), followed by incubation with HRP-conjugated anti-mouse IgG antibody. The assays were developed with the Vector VIP peroxidase substrate kit (Vector Laboratories; catalog no. SK- 4600) according to the manufacturer's instructions. The viral titers were expressed in focus-forming units (FFU) per milliliter.

2.2. Mouse Brain Slices Culture and Infection

CD1 IGS mice were purchased from Charles River. The care and use of these mice were strictly controlled according to european and national regulations for the protection of vertebrate animals used for experimental and other scientific purposes. Coronal slices from E15 embryos were sectioned at 300 μm on a Vibratome (Leica Microsystems) in artificial cerebrospinal fluid (ACSF) solution and then cultured in modified cortical culture medium (M-CCM) containing 71% basal MEM, 25% Hanks balanced salt solution, 2% FBS, 1% N-2 supplement (Thermo Scientific), 1× penicillin/streptomycin/glutamine (GIBCO BRL), and 0.66% glucose. Slices remained incubated in 5% CO_2 at 37 °C. Mice embryonic brain slices were infected with 6.10^5 FFU in 200 μL medium. After 2 h at 37 °C, the inoculum was replaced with 200 μL of fresh M-CCM. The slices were then incubated at 37 °C and fixed with 400 μL of 4% paraformaldehyde for 2 h at 4 °C.

2.3. Immuno-staining and Imaging

Brain slices were washed with PBS and stained in PBS, 0.3% Triton X-100 supplemented with donkey serum. Primary antibodies were incubated overnight at 4 °C and secondary antibodies were incubated for 2 h at room temperature. Brain slices were mounted with a small piece of double-sided tape on either side of the slide to act as a small scaffold for the coverslip. Imaging was performed using a spinning disk microscope equipped with a Yokogawa CSU-W1 scanner unit. Antibodies used in this study were: mouse anti-E glycoprotein (4G2) (RD-Biotech); rabbit anti-NeuN (Abcam); rabbit anti-Pax6 (Biolegend); rabbit anti-cleaved caspase 3 (Cell signaling) and goat anti-phospho-Histone 3 (Santa Cruz).

3. Results

To better understand how ZIKV infection may lead to microcephaly, we developed an assay to infect cultured mouse embryonic brain slices and tested the ability of ZIKV and other flaviviruses to infect the neocortex (Fig. 1a). We selected an isolate of DENV serotype 4 (DENV-4), responsible for a lethal fulminant hepatitis (Kudelko et al., 2012) and the encephalitic West Nile virus (WNV) Israel 1998 strain (IS98) (Lucas et al., 2004). Importantly, ZIKV infection was performed using the microcephaly-associated French Polynesian 2013 strain (Pf13) which is over 97% identical at the nucleotide level to the Brazilian strain but phylogenetically more distant from the African lineage (Zhu et al., 2016) (Fig. 1b). E15 mouse embryonic brains were sliced and cultured in modified cortical culture medium (M-CCM) (Baffet et al., 2016) and brain slices were infected for 2 h with either virus produced on C6/36 mosquito cells (6.10^5 FFU). Viral input was then removed and brain slices cultivated for 24 to 48 h at 37 °C (Fig. 1a). Viral titration revealed productive infection of ZIKV and WNV after 24 and 48 h, but not of DENV-4, indicating that the mouse developing neocortex is able to support replication of these two viruses (Fig. 1c). Immuno-staining experiments confirmed that ZIKV and WNV efficiently infect E15 brain slices whereas no cells infected by DENV-4 were detected (Fig. 1d). Interestingly ZIKV and WNV showed very different distributions. While WNV was distributed throughout the developing neocortex with enrichment in the intermediate zone (IZ) and cortical plate (CP), ZIKV was strongly concentrated in the ventricular zone (VZ) (Fig. 1d). Moreover, ZIKV-infected cells exhibited a characteristic RGP cell morphology, with an apical and a basal process running all the way up to the pial surface (Fig. 1e,

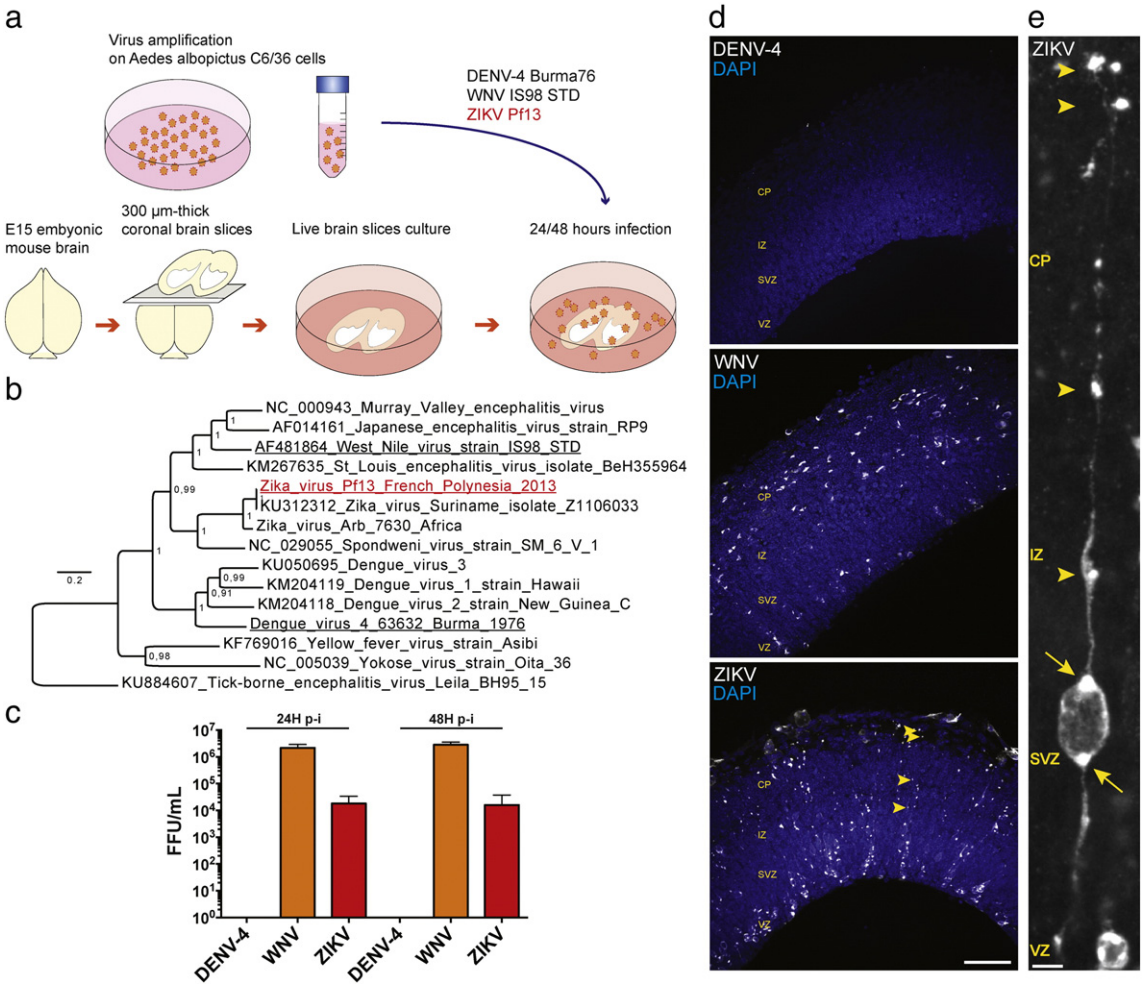

Fig. 1. Mouse cortical brain slices sustain ZIKV and WNV, but not DENV4 replication. a. Schematic representation of experimental approach. E15 mouse embryonic brains are sliced and cultured in modified cortical culture medium. Brain slices are then infected for 2 h with ZIKV, WNV and DENV-4 (6.10^5 FFU), all produced on C6/36 mosquito cells. Viruses are then washed out and brain slices cultivated for 24 to 48 h. b. Maximum likelihood phylogenetic tree inferred for sequences from NS5 genes of *Flavivirus* genus. The tick-borne encephalitis lineage was used as outgroup to root the tree. Viruses used in this study are underlined, ZIKV Pf13 strain is highlighted in red. c. Viral titration: supernatants were collected from previously infected brain slices and viral titers were quantified by focus forming assay (FFA) in Vero NK cells 24 and 48-hours post-infection. Error bars represent the standard deviations of results from three independent experiments (for each experiment, assays were performed in triplicate). d. Mouse embryonic brain slices infected at E15 with DENV-4, WNV or ZIKV, fixed after 24 h and immun-ostained with pan-flavivirus antibody directed against the E glycoprotein (4G2). VZ: ventricular zone; SVZ: sub-ventricular zone; IZ: intermediate zone; CP: cortical plate. Scale bar: 50 µm. e. High magnification image of a single ZIKV-infected cell in the VZ reveals clear radial glial morphology, with an apical process in contact with the ventricular surface and a basal process that extends all the way to the pial surface. Two viral factories can be observed in the perinuclear region. Scale bar: 5 µm. For each experiment, at least three infections were performed.

arrowheads mark basal processes). Viral factories could be observed, most often located in the perinuclear region (Fig. 1e, arrows).

To confirm this differential tropism of infection between ZIKV and WNV, we performed cell fate analysis. Quantification of Pax6+ infected cells revealed that the vast majority of ZIKV-infected cells were indeed RGP cells (84.9% ± 7.6%, n = 2612 cells) (Fig. 2a, c). Conversely, only 29.7% ± 4.8% of WNV-infected cells were Pax6+ RGP cells (n = 4370 cells) (Fig. 2a, c). Consistent with these results, only 10.76% ± 1.67% of ZIKV-infected cells were NeuN+ neurons (n = 3281 cells), *versus* 74.6% ± 5.6% of WNV-infected cells (n = 4287 cells) (Fig. 2b, d). At this stage the ratio between these two cell types was 1.69 ± 0.2 neuron for 1 RGP cell (Fig. 2e), indicating that the strong ZIKV tropism of infection for RGP cells was not merely due to their higher abundance. Next we asked if ZIKV infection affected proliferation and survival of RGP cells. Immuno-staining of mitotic Pax6+ RGP cells using anti-phospho Histone H3 antibody (pH3) revealed a mitotic index of 3.97% ± 0.16% for noninfected cells (n = 10,121 cells), consistent with previously reported measurements (Hu et al., 2013) (Fig. 3a, c). This value was not significantly affected after WNV infection (4.01% ± 0.39%, n = 4422 cells). However, ZIKV infection strongly reduced mitotic index (1.19% ± 0.33%, n = 4115 cells), indicating that ZIKV, but not WNV, impairs cell cycle progression of RGP cells (Fig. 3a, c). Cleaved caspase 3 staining (Cas3) did not reveal increased apoptotic cell death after infection with ZIKV or WNV (Fig. 3b, d). In fact, these viruses both appeared to inhibit apoptosis 24-h post-infection, consistent with the anti-apoptotic activity of flaviviruses in the early stages of infection (Lee et al., 2005).

4. Discussion

In this study, we describe the infection pattern of ZIKV and other closely related flaviviruses in the developing brain. Our results indicate that ZIKV infection exhibits a striking bias towards RGP cells and strongly impairs their proliferation, suggesting a potential route leading to microcephaly. Importantly, we did not observe this preferential infection of RGP cells for neurotropic WNV, while DENV-4 does not infect the neocortex at all. Recent evidence revealed absence of placenta infection by DENV-3 after inoculation into pregnant mice (Miner et al., 2016), supporting the notion that dengue viruses may represent a useful comparison point to identify ZIKV-specific infection routes. How ZIKV enters

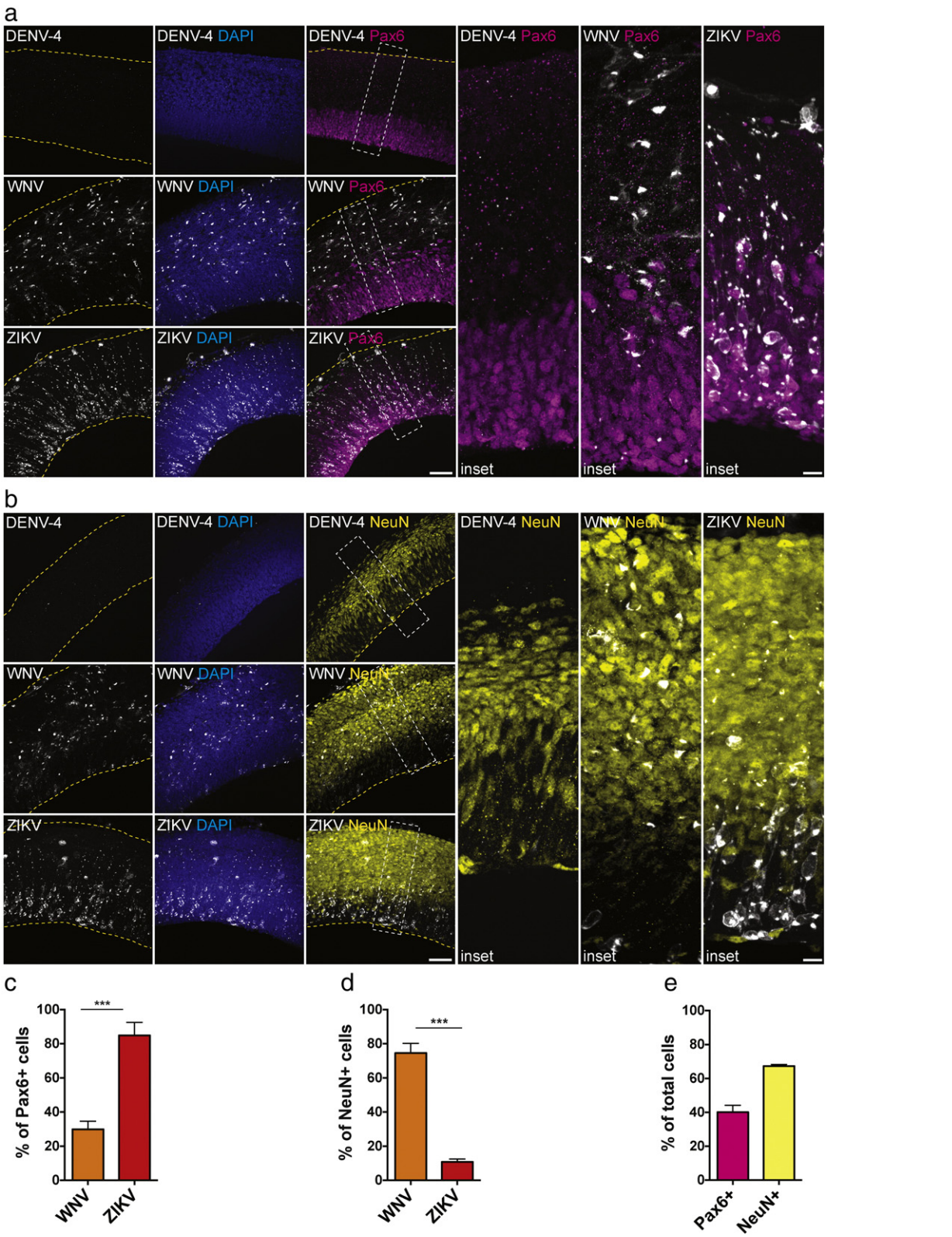

Fig. 2. ZIKV, DENV-4 and WNV tropism of infection in the developing neocortex. a. Mouse embryonic brain slices infected with DENV-4, WNV or ZIKV and stained for RGP cell marker Pax6. Scale bars: 50 μm and 10 μm for insets. b. Mouse embryonic brain slices infected with DENV-4, WNV or ZIKV and stained for neuronal marker NeuN. Scale bars: 50 μm and 10 μm for insets. c. Quantification of the percentage of WNV- and ZIKV-infected cells positive for RGP cell marker Pax6 reveals strong preferential infection of these cells by ZIKV, but not by WNV. All infected cells within the first 50 μm of each brain slice were counted. d. Quantification of the percentage of WNV- and ZIKV-infected cells positive for neuronal marker NeuN reveals preferential infection of these cells by WNV, but not by ZIKV. e. Quantification of the percentage of Pax6+ and NeuN+ cells in non-infected E15 brain slices, cultivated for 24 h. For each experiment, at least three infections were performed. Error bar indicate SD. ***$p < 0.005$ based on a Student's *t*-test.

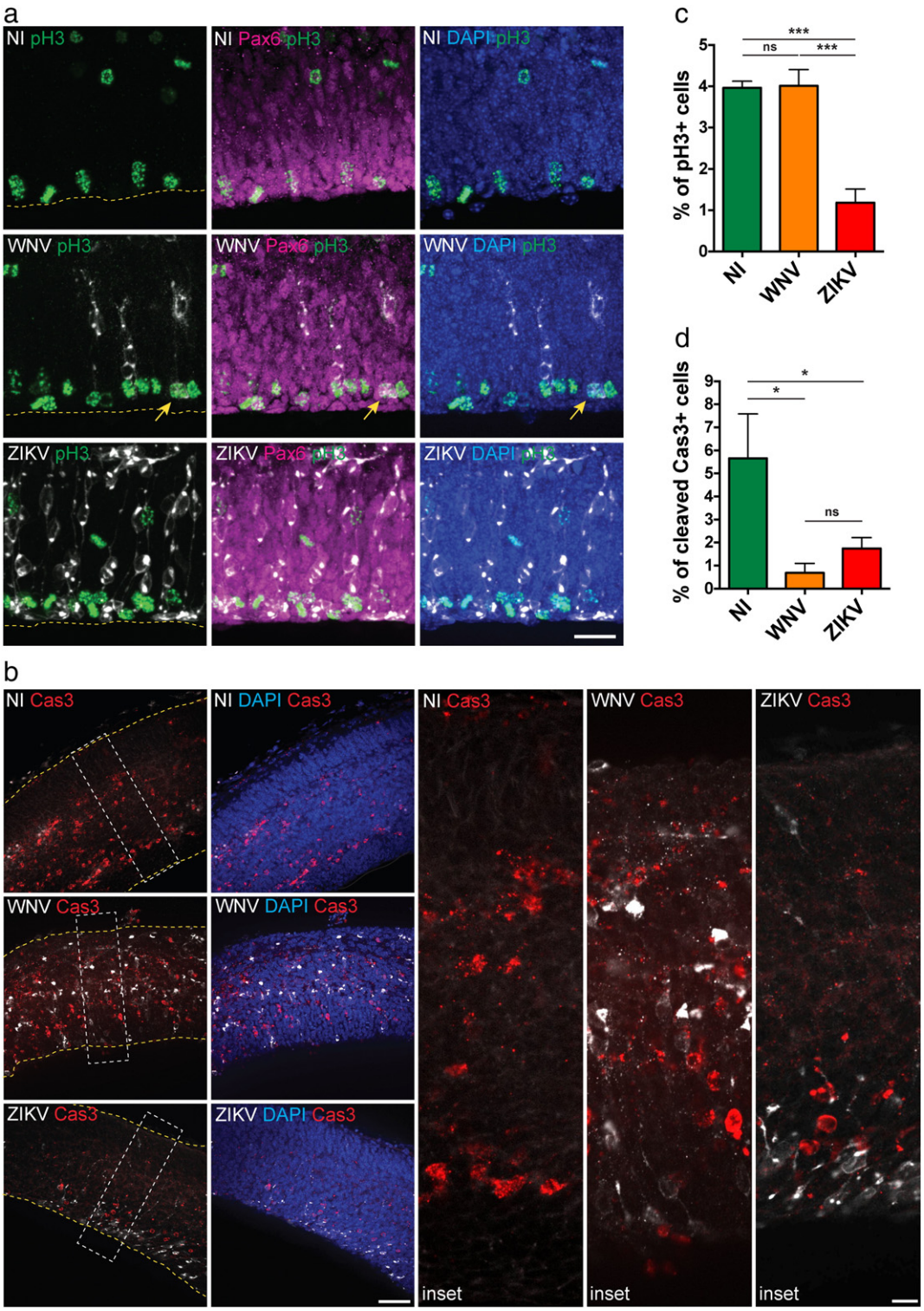

Fig. 3. ZIKV and WNV effect on cell cycle progression and apoptosis. a. Mouse embryonic brain slices infected with WNV, ZIKV or non-infected (NI) and stained for RGP cell marker Pax6 and mitotic marker phospho-Histone 3 (pH3). Yellow arrow indicates mitotic WNV-infected cell. Scale bar: 20 μm. b. Mouse embryonic brain slices infected with WNV, ZIKV or non-infected (NI) and stained for apoptotic marker cleaved caspase-3 (Cas3). Scale bars: 50 μm and 10 μm for insets. c. Quantification of the percentage of mitotic cells (pH3+) out of total RGP cells (Pax6+) reveals strong cell cycle progression defects in ZIKV-infected cells but not in WNV-infected cells. d. Quantification of the percentage of apoptotic cells (Cas3+) out of total cells reveals decreased apoptosis in ZIKV (n = 3655 cells) and WNV-infected cells (n = 6644 cells), as compared to non-infected cells (n = 35,829 cells). For each experiment, at least three infections were performed. Error bar indicate SD. *$p < 0.05$; ***$p < 0.005$; ns, not significant, based on a Student's *t*-test.

RGP cells is still unclear but recent observations showed strong expression of the candidate entry receptor AXL in mice and human RGP cells (Nowakowski et al., 2016).

Our analysis revealed that ZIKV strongly impairs cell cycle progression of RGP cells, consistent with recent reports (Qian et al., 2016; Li et al., 2016). Surprisingly, WNV-infected RGP cells did not show such

cell cycle abnormalities. Our comparative analysis should therefore prove very powerful to identify the molecular pathways responsible for ZIKV's specific anti-mitotic activity. It will also be important to test if non-microcephaly-associated ZIKV strains from the African lineage may have different effect and tropism of infection in the developing neocortex, compared to the Pf13 strain from the Asian lineage used in this study (Cugola et al., 2016).

We focused here on the early stages of neocortex infection (24 h, representing a full replication cycle of the virus) and observed a reduction of apoptotic cell death, which may represent a crucial step for ZIKV infection of the developing brain. Recent studies have reported increased apoptosis several days post-infection with ZIKV (Li et al., 2016; Qian et al., 2016; Garcez et al., 2016). The development of methods to cultivate infected brain slices for multiple days (5–7 days) will therefore be critical to identify the long-term consequences of ZIKV infection and to describe if a switch from reduced to increased apoptosis indeed occurs during the course of ZIKV infection.

Our work establishes a framework to identify ZIKV-specific processes leading to microcephaly. While our approach does not address the critical steps by which the virus reaches the brain, it allows to precisely characterize the molecular and cellular alterations caused by different flaviviruses. We show that ZIKV, but not other closely related flaviviruses, has a strong tropism of infection for the neural stem cells. ZIKV impairs cell cycle progression of neural stem cells and inhibits apoptotic cell death at early stages of brain infection, which may represent two crucial events in the route leading to microcephaly. The development of similar assays to infect human fetal developing brain is now of urgent need and will be crucial to fully understand congenital Zika syndrome (Check Hayden, 2016).

Acknowledgments & Funding

We are grateful to Joseph J. Cockburn and Renata Basto for helpful comments and suggestions on the manuscript. We thank Valérie Caro, Laure Diancourt and Meriadeg Ar Gouilh for assistance with the phylogenetic tree. The Baffet and Goud labs are part of the Labex CelTisPhyBio (11-LBX-0038) and the Idex Paris Sciences et Lettres (ANR-10-IDEX-0001-02 PSL). Seventh Framework Programme (FP7) provided funding under grant number 278433-PREDEMICS to NP, JB and MPF. Ministry of Defence/Direction Générale de l'Armement (DGA) provided funding to CK. This work was supported by the European Research Council advanced grants (project 339847 'MYODYN' to B.G.). We acknowledge the Curie Cell and Tissue Imaging Platform—PICT-IBiSA (member of France–Bioimaging) for technical assistance.

Conflict of Interest Statement

The authors declare no conflict of interest.

Author Contribution

ADB, NP and JBB designed the study. NP, CK, JB and MPF prepared virus stocks, performed infections and viral titrations. ADB prepared brain slices. ADB, JBB and LC performed immuno-staining experiments, acquired images at the microscope, analyzed and quantified the data. VF provided assistance with image acquisition. ADB, NP and JBB wrote the manuscript.

References

Alsaleh, K., et al., 2016. The E glycoprotein plays an essential role in the high pathogenicity of European-Mediterranean IS98 strain of West Nile virus. Virology 492, 53–65.
Baffet, A.D., et al., 2016. Cellular and subcellular imaging of motor protein-based behavior in embryonic rat brain. Methods Cell Biol. 131, 349–363.
Barkovich, A.J., et al., 2012. A developmental and genetic classification for malformations of cortical development: update 2012. Brain 135 (Pt 5), 1348–1369.
Calvet, G., et al., 2016. Detection and sequencing of Zika virus from amniotic fluid of fetuses with microcephaly in Brazil: a case study. Lancet Infect. Dis.
Cao-Lormeau, V.-M., et al., 2014. Zika virus, French Polynesia, South Pacific, 2013. Emerg. Infect. Dis. 20 (6), 1085–1086.
Cauchemez, S., et al., 2016. Association between Zika virus and microcephaly in French Polynesia, 2013–15: a retrospective study. Lancet (Lond. Engl.) 387 (10033), 2125–2132.
Chaturvedi, U.C., et al., 1980. Transplacental infection with Japanese encephalitis virus. J. Infect. Dis. 141 (6), 712–715.
Check Hayden, E., 2016. Zika highlights role of controversial fetal-tissue research. Nature 532 (7597), 16.
Cugola, F.R., et al., 2016. Not final proof. Nature 1–15.
Dang, J., et al., 2016. Zika virus depletes neural progenitors in human cerebral organoids through activation of the innate immune receptor TLR3. Cell Stem Cell http://dx.doi.org/10.1016/j.stem.2016.04.014.
Dick, G.W.A., Kitchen, S.F., Haddow, A.J., 1952. Zika virus. I. Isolations and serological specificity. Trans. R. Soc. Trop. Med. Hyg. 46 (5), 509–520.
Fernández, V., Llinares-Benadero, C., Borrell, V., 2016. Cerebral cortex expansion and folding: what have we learned? EMBO J.
Garcez, P.P., et al., 2016. Zika virus impairs growth in human neurospheres and brain organoids. Science 352 (6287), 816–818.
Heymann, D.L., et al., 2016. Zika virus and microcephaly: why is this situation a PHEIC? Lancet (Lond. Engl.) 387 (10020), 719–721.
Hu, D.J.-K., et al., 2013. Dynein recruitment to nuclear pores activates apical nuclear migration and mitotic entry in brain progenitor cells. Cell 154 (6), 1300–1313.
Kriegstein, A.R., Alvarez-Buylla, A., 2009. The glial nature of embryonic and adult neural stem cells. Annu. Rev. Neurosci. 32, 149–184.
Kudelko, M., et al., 2012. Class II ADP-ribosylation factors are required for efficient secretion of dengue viruses. J. Biol. Chem. 287 (1), 767–777.
Lee, C.J., Liao, C.L., Lin, Y.L., 2005. Flavivirus activates phosphatidylinositol 3-kinase signaling to block caspase-dependent apoptotic cell death at the early stage of virus infection. J. Virol. 79 (13), 8388–8399.
Li, C., et al., 2016. Zika virus disrupts neural progenitor development and leads to microcephaly in mice. Stem Cells 1–8.
Lucas, M., et al., 2004. The Israeli strain IS-98-ST1 of West Nile virus as viral model for West Nile encephalitis in the old world. Virol. J. 1, 9.
Martines, R.B., et al., 2016. Notes from the field: evidence of Zika virus infection in brain and placental tissues from two congenitally infected newborns and two fetal losses - Brazil, 2015. MMWR Morb. Mortal. Wkly Rep. 65 (6), 159–160.
Miner, J.J., et al., 2016. Zika virus infection during pregnancy in mice causes placental damage and fetal demise. Cell 1–12.
Mlakar, J., et al., 2016. Zika virus associated with microcephaly. N. Engl. J. Med. 374 (10), 951–958.
Neu, N., Duchon, J., Zachariah, P., 2015. TORCH infections. Clin. Perinatol. 42 (1), 77–103 (viii).
Nowakowski, T.J., et al., 2016. Expression analysis highlights AXL as a candidate Zika virus entry receptor in neural stem cells. Stem Cells 1–17.
O'Leary, D.R., et al., 2006. Birth outcomes following West Nile virus infection of pregnant women in the United States: 2003–2004. Pediatrics 117 (3), e537–e545.
Oliveira Melo, A.S., et al., 2016. Zika virus intrauterine infection causes fetal brain abnormality and microcephaly: tip of the iceberg? Ultrasound Obstet. Gynecol. 47 (1), 6–7.
Paixão, E.S., et al., 2016. History, epidemiology, and clinical manifestations of Zika: a systematic review. Am. J. Public Health 106 (4), 606–612.
Qian, X., et al., 2016. Brain-region-specific organoids using mini-bioreactors for modeling ZIKV exposure. Cell 165 (5), 1238–1254.
Rozé, B., et al., 2016. Zika virus detection in cerebrospinal fluid from two patients with encephalopathy, Martinique, February 2016. Euro Surveill. 21 (16).
Tang, H., et al., 2016. Zika virus infects human cortical neural progenitors and attenuates their growth. Stem Cells 1–5.
Taverna, E., Götz, M., Huttner, W.B., 2014. The cell biology of neurogenesis: toward an understanding of the development and evolution of the neocortex. Annu. Rev. Cell Dev. Biol. 30, 465–502.
Zhu, Z., et al., 2016. Comparative genomic analysis of pre-epidemic and epidemic Zika virus strains for virological factors potentially associated with the rapidly expanding epidemic. Emerg. Microbes Infect. 5, e22.